Mathematical Sciences Letters
An International Journal

http://dx.doi.org/10.18576/msl/070103

Dissipation Effect on MHD Stagnation-Point Flow of Casson Fluid Over Stretching Sheet Through Porous Media

Satya Ranjan Mishra[1], *Asmat Ara*[2,*] *and Najeeb Alam Khan*[3]

[1] Department of Mathematics, Institute of Technical Education and Research, Siksha Anusandhan University, Khandagiri, Bhubaneswar, Odisha 751030, India
[2] Department of Computer Science, Mohammad Ali Jinnah University, Karachi 75400, Pakistan
[3] Department of Mathematics, University of Karachi, Karachi 75270, Pakistan

Received: 28 Feb. 2017, Revised: 15 Sep. 2017, Accepted: 21 Sep. 2017
Published online: 1 Jan. 2018

Abstract: The present study analyses the stagnation-point flow over a stretching sheet embedded in a porous medium. The plane stagnation-point flow is a class of flow problem which involves two-dimensional flow. The present study develops a mathematical model of a non-Newtonian flow of Casson fluid. The novelty of the present study is to account for the effect of permeability of the medium as well as energy loss due to Julian dissipation. A linear Darcian model is used to model the flow through porous media, whereas the non-linear term in energy equation accounts for the Joulian dissipation. Some interesting outcomes of the present study are the presence of porous matrix, which enhances the velocity thereby contributing to the growth of boundary layer and accelerates the momentum diffusion through larger fluid layers, whereas Julian dissipation is counterproductive for the growth of thermal boundary layer i.e. moderately large Eckert number produces thinner boundary layer.

Keywords: Casson fluid, Stagnation-Point, Porous sheet, MHD flow, Runge-Kutta fourth order

1 Introduction

The exact solution of the flow problem in the vicinity of a stagnation-point for both two and three-dimensional flows of a viscous fluid may be obtained from the consideration that at large distances from the stagnation-point the flow is essentially same as that of the corresponding potential flow problem. Thus, the solution of viscous flow may be derived from the solution of the potential flow problem. The study of stagnation-point flow over a stretching sheet has attracted many researchers [1,2,3,4,5]. This problem holds numerous applications such as glass fiber, cooling of a metallic plate, polymer-processing manufacturing of glass sheets, paper production, and many others. Crane [1] initiated a study of viscous fluid towards a linearly stretching sheet. Caragher and Crane [2] analyzed heat transfer aspect on a continuous stretching sheet. The use of similarity transformation in solving flow and heat transfer equation is one of the most successful idealization in fluid mechanics [3]. An exact similarity solution for the dimensionless differential system of the flow model has been obtained. Many investigations have been carried out to examine the flow over a stretching/shrinking sheet under different aspects of magnetohydrodynamic (MHD), suction/injection, heat and mass transfer etc. [4,5,6,7,8,9,10,11]. Magnetohydrodynamic three-dimensional flow and heat transfer over a stretching surface in a viscoelastic fluid were discussed by Ahmad and Nazar [12]. Recently, in another article, Nadeem et al. [13] examined the magnetohydrodynamic boundary layer flow of a Casson fluid over an exponentially accelerated shrinking sheet. They discussed the analytical solutions of the differential system by Adomian decomposition method (ADM). Mishra et al. [14] investigated the mass and heat transfer effect on MHD flow of a viscoelastic fluid through a porous medium with oscillatory suction and heat source.

The flow and heat transfer of Jeffrey fluid near stagnation-point on a stretching/shrinking sheet with the parallel external flow was investigated by Turkyilmazoglu

* Corresponding author e-mail: noble.asmat@yahoo.com

and Pop [15]. They developed an exact solution to the Navier-Stokes equations. Chiam [16] studied the combined problem of Hiemenz [17] and Crane [1], i.e. the stagnation-point flow over a stretching sheet where they considered the identical stretching velocity and straining velocity and found no boundary layer structure near the sheet. Afterward, Mahapatra and Gupta [18] re-investigated the stagnation-point flow towards a stretching sheet taking different stretching and straining velocities and ultimately they found two different kinds of boundary layer structures near the sheet depending on the ratio of the stretching and straining velocity rates. However, some other important investigations concerning the stagnation-point flow over stretching sheet were made by Mahapatra and Gupta [19], Fredrickson [20] investigated the steady flow of a Casson fluid in a tube. The unsteady boundary layer flow and heat transfer of a Casson fluid over a moving flat plate with a parallel free stream were studied by Mustafa et al. [21] and they solved the problem analytically by using homotopy analysis method (HAM). Bhattacharyya et al. [22,23] reported the exact solution for boundary layer flow of Casson fluid over a permeable stretching/shrinking sheet with and without external magnetic field. Recently, Bhukta et al. [24] have studied heat and mass transfer on the MHD flow of a Viscoelastic fluid through porous media over a shrinking sheet. Entropy analysis for an unsteady MHD flow past a stretching permeable surface in nanofluid was investigated by Abolbashari et al. [25]. Rashidi et al. [26] studied the mixed convective heat transfer for MHD viscoelastic fluid flow over a porous wedge with thermal radiation. Further Rashidi and Erfani [27] have studied steady MHD convective and slip flow due to a rotating disk with viscous dissipation and Ohmic heating and solve the same problem analytically. Recently, Freidoonimehr et al. Numerical and analytical solutions for Falkner-Skan flow of MHD Oldroyd-B fluid was investigated by Abbasbandy et al. [29].

It is well known that Casson fluid is a shear thinning liquid which is assumed to have an infinite viscosity at zero rates of shear, a yield stress below which no flow occurs and a zero viscosity at an infinite rate of shear, i.e. if a shear stress less than the yield stress is applied to the fluid, it behaves like a solid, whereas if a shear stress greater than yield stress, it starts moving [30]. The examples of Casson fluid are as follows: jelly, tomato sauce, honey, soup, concentrated fruit juices, etc. Human blood can also be treated as Casson fluid. Due to the presence of several substances like protein, fibrinogen, and globulin in aqueous base plasma, human red blood cells can form a chainlike structure, known as aggregates or rouleaux. If the rouleaux behaves like a plastic solid, then there exists a yield stress that can be identified with the constant yield stress in Casson fluid [31].

The objective of the present study is to generalize the works of Nazar et al. [32] and Bhattacharyya [33] by incorporating the loss due to Julian dissipation in the energy equation. Moreover, the flow is subjected to pass through a porous medium, which has been effectively accounted with the help of a non-Darcy model. The extension is justified as because no system is foolproof to trap the thermal energy loss. Secondly, the flow through a porous media is more practical having numerous applications in the field of oil recovery and saline aquifer.

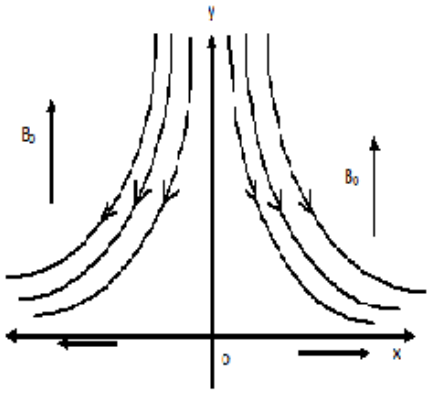

Fig. 1: Flow Geometry

2 Mathematical Analysis

Consider the flow of an incompressible Casson fluid past a flat sheet that coincides with the plane $y = 0$. The fluid flow is confined to $y > 0$. Two equal and opposite forces are applied along x-axis to initiate the formation of the fluid. The rheological equation of state for an isotropic and incompressible flow of Casson fluid is as follows:

$$\tau_{ij}(x) = \begin{cases} 2(\mu_B + \frac{p_y}{\sqrt{2\pi}})e_{ij} & \pi > \pi_c, \\ 2(\mu_B + \frac{p_y}{\sqrt{2\pi_c}})e_{ij} & \pi < \pi_c \end{cases} \tag{1}$$

The governing continuity, momentum, and energy equations of such type of flow following Bhattacharyya [33] are written as:

$$\frac{\partial u}{\partial x} + \frac{\partial v}{\partial y} = 0, \tag{2}$$

$$u\frac{\partial u}{\partial x} + v\frac{\partial v}{\partial y} = U_s\frac{dU_s}{dx} + \nu\left(1 + \frac{1}{\beta}\right)\frac{\partial^2 u}{\partial y^2} - \left(\frac{\sigma {B_0}^2}{\rho} + \frac{\nu}{k_p}\right)(u - U_s), \tag{3}$$

$$u\frac{\partial T}{\partial x} + v\frac{\partial T}{\partial y} = \frac{k}{\rho c_p}\frac{\partial^2 T}{\partial y^2} - \frac{1}{\rho c_p}\frac{\partial q_r}{\partial y} - \frac{\sigma B_0^2}{\rho}u^2. \tag{4}$$

Table 1: Nomenclature

a	Straining rate parameter $[s^{-1}]$	B	Velocity ratio parameter
c	Stretching constant	C_f	Wall skin friction coefficient
c_p	Specific heat [J/(Kg.K)]	ψ	Dimensionless stream function
B_0	Strength of magnetic field $[kgs^{-2}A^{-1}]$	k_p	Porosity parameter
M	Magnetic parameter	E_c	Eckert number
P_r	Prandtl number	Nu_x	Local Nusselt number
p_y	Stress of fluid $[kgm^{-1}s^{-2}]$	q_r	Radiative heat flux $[Wm^{-2}]$
q_w	Heat flux from the sheet	R	Thermal radiation parameter
Re_x	Local Reynolds number	T	Temperature $[K]$
T_w	Constant temperature at the sheet [K]	T_∞	Free stream temperature $[K]$
U_s	Straining velocity $[ms^{-1}]$	U_w	Stretching velocity of the sheet $[ms^{-1}]$
u, v	Velocity components $[ms^{-1}]$	e_{ij}	(i, j)th component of deformation rate
Greek symbols			
β	Non-Newtonian Casson parameter	δ	Velocity boundary layer thickness [m]
η	Similarity variable	η_∞	Finite value of η
k	Thermal conductivity $[Wm^{-1}K^{-1}]$	π	Product of the components
π_c	Critical value of π	υ	Kinematic fluid viscosity $[m^2s^{-1}]$
ρ	Fluid density $[kgm^{-3}]$	ψ	Stream function
τ_w	Shear stress $[kgm^{-1}s^{-2}]$	σ^*	Stefan ? Boltzmann constant $[Wm^{-2}K^{-4}]$
μ_B	Plastic dynamic viscosity $[kgm^{-1}s^{-1}]$	θ	Dimensionless temperature [K]
σ	Electrical conductivity of the fluid $[s^3A^2kg^{-1}m^{-3}]$		

The appropriate boundary conditions are:

$$\left.\begin{array}{ll} u = U_w,\ v = 0,\ T = T_w & \text{at } y = 0, \\ u \to U_s,\ T \to T_\infty & \text{as } y \to \infty \end{array}\right\} \tag{5}$$

Where, u and v are the velocity components in x and y directions respectively. $U_s = ax$ is the straining velocity of the stagnation-point with $a(>0)$ being the straining constant and $U_w = cx$ is the stretching velocity of the sheet with $c(>0)$ being the stretching constant.
The equation of continuity Eq. (2) is identically satisfied if we take the stream function $\psi(x,y)$ such that:

$$u = \frac{\partial \psi}{\partial y},\ v = -\frac{\partial \psi}{\partial x} \tag{6}$$

Using Eq. (6), the momentum equation, Eq. (3) takes the form:

$$\frac{\partial \psi}{\partial y}\frac{\partial^2 \psi}{\partial x \partial y} - \frac{\partial \psi}{\partial x}\frac{\partial^2 \psi}{\partial y^2} = U_s\frac{dU_s}{dx} + \nu\left(1+\frac{1}{\beta}\right)\frac{\partial^3 \psi}{\partial y^3} - \left(\frac{\sigma B_0^2}{\rho} + \frac{\nu}{k_p}\right)\left(\frac{\partial \psi}{\partial y} - U_s\right) \tag{7}$$

The boundary condition in Eq. (5) reduces to:

$$\begin{array}{ll} \dfrac{\partial \psi}{\partial y} = U_w,\ \dfrac{\partial \psi}{\partial x} = 0, & \text{at } y = 0, \\ \dfrac{\partial \psi}{\partial y} \to U_s, & \text{as } y \to \infty \end{array} \tag{8}$$

Using the Rosseland approximation, the radiation parameter is $q_r = -\frac{4\sigma^*}{3k_1}\frac{\partial T^4}{\partial y}$, where σ^* is the Stefan-Boltzmann constant and k_1 is the absorption coefficient. Using Taylor's series to expand T^4 about T_∞ and neglecting higher-order terms, we get $T^4 = 4T_\infty{}^3T - 3T_\infty{}^4$.

Now Eq. (4) becomes:

$$u\frac{\partial T}{\partial x} + v\frac{\partial T}{\partial y} = \frac{k}{\rho c_p}\frac{\partial^2 T}{\partial y^2} + \frac{16\sigma T_\infty^3}{3k_1\rho c_p}\frac{\partial^2 T}{\partial y^2} - \frac{\sigma B_0^2}{\rho}u^2 \tag{9}$$

The momentum and energy equations, Eqs. (7) and (9) can be transformed into the corresponding ordinary differential equations by introducing the following similarity transformations:

$$\psi(x,y) = \sqrt{c\nu}xf(\eta),$$
$$\frac{T-T_\infty}{T_w-T_\infty} = \theta(\eta) \tag{10}$$

where $\eta = y\sqrt{\frac{c}{\nu}}$
The momentum and energy equations, Eqs. (7) and (9) are transformed to:

$$\left(1+\tfrac{1}{\beta}\right)f''' + ff'' - f'^2 - \left(M + \tfrac{1}{k_p}\right)(f' - B) + B^2 = 0,$$
$$(3R+4)\theta'' + 3RP_r f\theta' - 3RP_rME_c f'^2 = 0 \tag{11}$$

The non-dimensional parameters are:

$$M = \frac{\sigma B_0^2}{\rho c},\ B = \frac{a}{c},\ P_r = \frac{c\mu}{k},$$
$$E_c = \frac{1}{c_{p(T_w - T_\infty)}} c^2 x^2,\ R = \frac{k^* k_1}{4\sigma T_\infty^3}$$

Subject to the boundary conditions:

$$\left.\begin{array}{ll} f(\eta) = 0,\ f'(\eta) = 1,\ \theta(\eta) = 0 & \text{at } \eta = 0, \\ f'(\eta) \to B,\ \theta(\eta) \to 0 & \text{as } \eta \to \infty \end{array}\right\} \quad (12)$$

3 Numerical Method

The set of coupled non-linear governing boundary layer equations, Eqs. (2) - (4) together with the boundary conditions in Eq. (5) are solved numerically by using Runge-Kutta method along with a shooting technique. First of all, higher order non-linear differential equations, Eqs. (2) - (4) are converted into a set of simultaneous non-linear differential equations of first order and they are further transformed into initial value problem by applying the shooting technique. The transformed initial value problem is solved by employing Runge-Kutta fourth order method. The step-size $\triangle\ \eta = 0.05$ is used to obtain the numerical solution with five decimal places of accuracy as the criterion of convergence. The aforesaid differential equations are written as follows:

$$f = y_1,\ f' = y_2,\ f'' = y_3,\ \theta = y_4,\ \theta' = y_5,$$

$$f''' = \frac{1}{1+\frac{1}{\beta}}\left(-y_1 y_3 + y_2^2 + \left(M + \frac{1}{k_p}\right)(y_2 - B) - B^2\right)$$

$$\theta'' = -\frac{1}{3R+4}(3RP_r M E_c y_2^2 - 3RP_r y_1 y_5)$$

$$y_1(0) = 0,\ y_2(0) = 1,\ y_4(0) = 1$$

In order to integrate we require with $y_3(0)$, $y_5(0)$, but these values are not given in the boundary condition. The suitable values of $y_3(0)$, $y_5(0)$ are chosen and integration is performed.

In course of numerical computation, the skin-friction coefficient and the Nusselt number that are respectively proportional to $f''(0), \theta'(0)$ are also calculated and their numerical values are presented in Table 2.

4 Results and Discussion

The following discussion is based on the numerical solution of both the boundary layer equations i.e. velocity boundary layer and thermal boundary layer. At the beginning, the validity check is carried out by comparing the present result with the work of Bhattacharyya [33] (without the porous medium and Julian dissipation). The specialty of the present study is to highlight the effect of porous medium and Julian dissipation on the stagnation-point flow of Casson fluid. From Eq. (12), it can be seen that the importance of Julian heating can be indicated by the combined effect of the magnetic parameter M and Eckert number E_c. The Eckert number is a measure of dissipation effect in the flow. Since this grows in proportion to the square of the velocity, it can be neglected for small velocities.

Fig. 2 exhibits the effect of velocity ratio in the porous and non-porous medium. For the purpose of comparison with Bhattacharyya, the dotted curve for $K_p = 10$, $B = 2.0$, $M = 0.5$, $\beta = 2$ is drawn. It is seen that the curve coincides with the curve presented in Fig. 1 of Bhattacharyya [33]. It is interesting to note that the velocity profile clearly displays three distinct characteristics for the ratio of straining and stretching i.e. $B < 1$, $B = 1$ and $B > 1$. $B = 1$ implies the equality of straining velocity of the stagnation point flow and stretching velocity of the sheet, which amounts to no motion. Therefore, the velocity remains constant throughout. On the other hand, $B > 1$ represents the dominance of straining over stretching, which leads to the increasing velocity in the layer close to bounding surface i.e. stretching sheet, thereafter the velocity remains constant. Moreover, it is seen that the effect of porous matrix is to increase the velocity profile. Further, it is seen that the profiles for $B < 1$ and $B > 1$ are almost symmetrical about $B = 1$. This means a three-layer character for $B < 1$, $B = 1$ and $B > 1$.

Fig. 3 and Fig. 4 exhibit the velocity variation for various values of the parameter β showing the characteristics of Casson fluid. It is to note that an increase in β leads to increasing the velocity in both the cases i.e. in the presence of porous medium and without it. Thus, it is concluded that the non-Newtonian property of Casson fluid model is responsible for diffusing the momentum through more number of layers of fluid contributing to thickening of boundary layer when the effect of straining dominates over stretching ($B > 1$). For $B < 1$, the profiles are a mirror image of $B > 1$ about the profile $B = 1$. Further, it is to note that the effect of Lorentz force is to reduce the velocity at all points. This is due to the resistive property of the ponderomotive force generated due to the interaction of magnetic field with conducting fluid (Fig. 4). On careful observation, it is further revealed that slight change in a magnetic field does not affect the velocity profile in both porous and nonporous media.

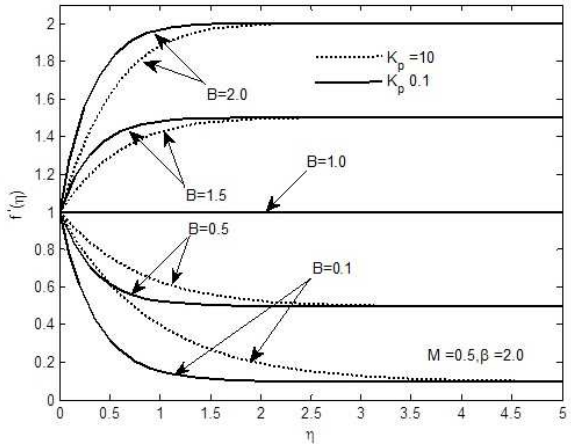

Fig. 2: Variation of B on velocity profile

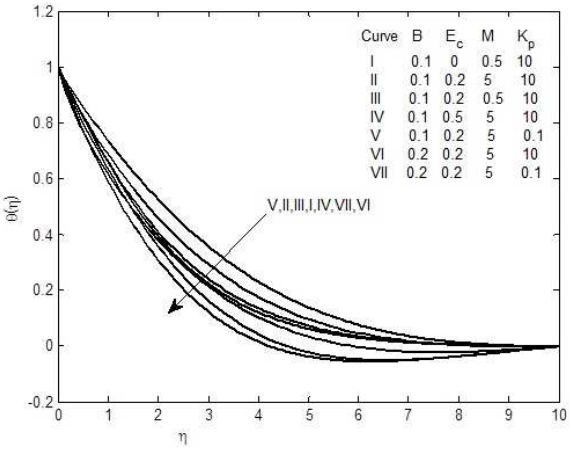

Fig. 5: Variation of B, E_c M and K_p on velocity profile

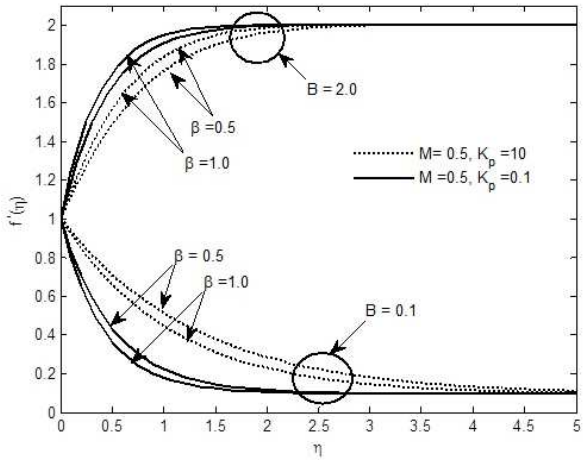

Fig. 3: Variation of β on velocity profile

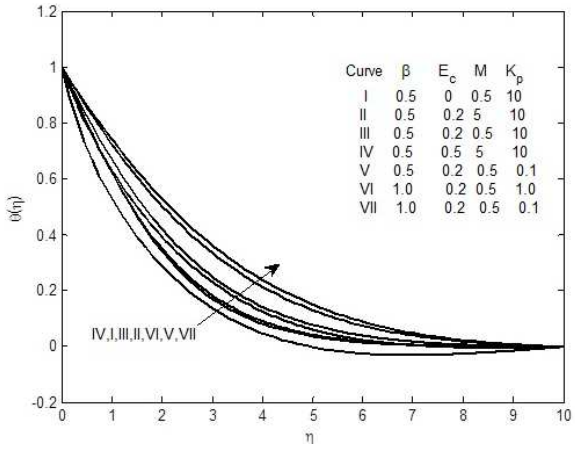

Fig. 6: Variation of β, E_c M and K_p on velocity profile

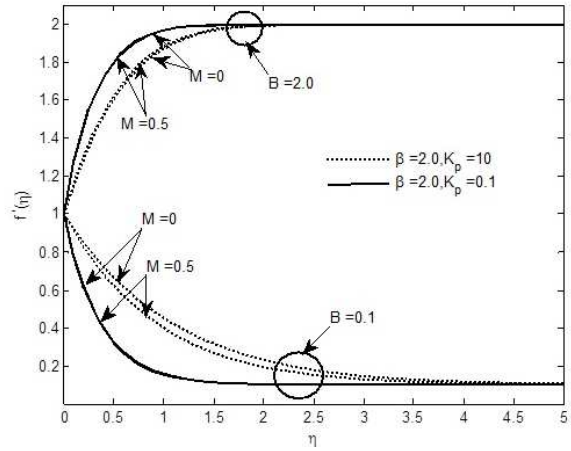

Fig. 4: Variation of M on velocity profile

Figs. 5- 7 are drawn when $P_r = 1$. P_r is the salient characteristic number. This imposes a pre-condition of equality and kinematic viscosity and thermal diffusivity. Figs. 5 and 6 depict the temperature variation for various values of characterizing parameters.

On careful observation, it is seen that decrease in M leads to decreasing the temperature at all layers (curves II and III) but the reverse effect is observed in the case of E_c (curves II and IV) as well as for B, $(B < 1)$ (curves II and VI). It is concluded that thinning of thermal boundary layer occurs due to higher thermal dissipation and stretching rate. It is also to noted that the presence of porous matrix increases the temperature. Moreover, (curves V and VII) of Fig. 6 show that non-Newtonian property of the Casson fluid enhances the temperature in the presence of porous matrix.

Fig. 7 (curve I) intends to present a very special case when the effects of magnetic field, dissipation, and

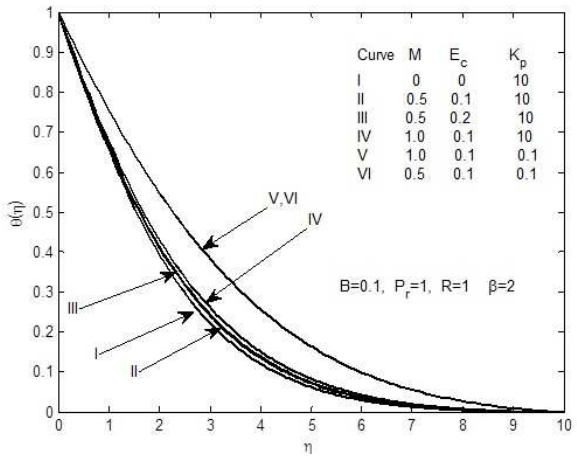

Fig. 7: Variation of M, E_c and K_p on velocity profile

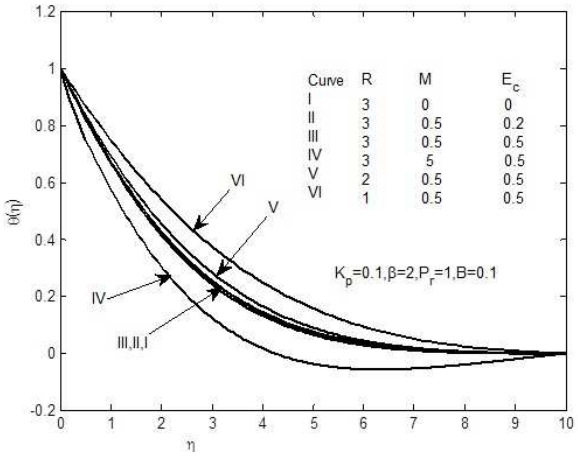

Fig. 9: Variation of R, M and E_c on velocity profile

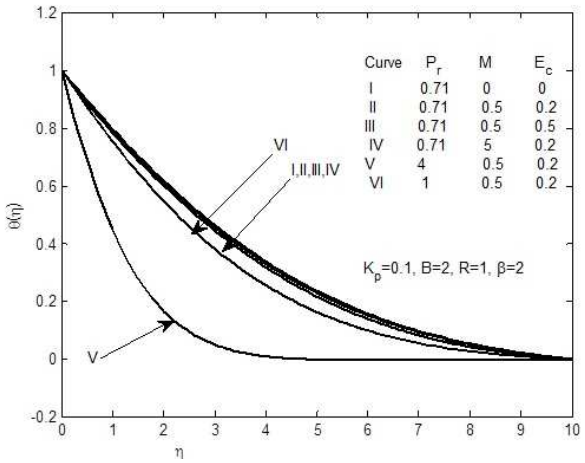

Fig. 8: Variation of P_r, M and E_c on velocity profile

Table 2: Values of $f''(0)$ for several values of B with $M = 0$ and $\beta = \infty$.

B	Nazar et al. [33]	Bhattacharyya et al. [33]	Present study
0.1	-0.9694	-0.969386	-0.969381
0.2	-0.9181	-0.918107	-0.918102
0.5	-0.6673	-0.667263	-0.667260
2	2.0176	2.017503	2.017486

porosity are absent. This leads to lower down the temperature which is otherwise established, in their presence, in earlier discussions.

Fig. 8 aims at showing the relative importance of kinematic viscosity and thermal diffusivity. It is evident that higher kinematic viscosity, in the case of liquid, restricts the heat transfer to fewer layers resulting in a thinner boundary layer, whereas for gas $P_r = 0.71$, the heat energy diffuses to larger layers.

Fig. 9 presents the effect of R, the radiation parameter. This shows that thermal radiation associated with magnetic effect lowers down the temperature (curves I and IV) when kinematic viscosity and thermal diffusivity enjoy the same order of priority.

Table 2 is prepared for validity and authenticity check by comparing the values of $f''^{(0)}$ with earlier works by Nazar et al. [32] and Bhattacharyya [33]. In the case of Newtonian fluid, this shows a good agreement. Table 3 presents the numerical values of surface criteria such as skin friction and Nusselt number. One most important finding is that skin friction assumes positive values for $B > 1$ i.e. $B = 2$ otherwise negative. This aspect has been clearly shown in the velocity graph. Thus the predominance of straining rate accounts for the positive values of skin friction. Therefore, straining rate and stretching rate have great influence on flow criteria including stability and growth of boundary layer. It is also noticed that all other parameters reduce the skin friction including Casson fluid parameter, which is desirable, except E_c, which has no significant effect.

Table 3 also focuses light on the Nusselt number, presenting rate of heat transfer at the bounding surface. It is evident that stretching rate ratio has no such effect as that of skin friction in reversing the rate of heat transfer at the surface. Further, it is to note that rate of heat transfer is enhanced with an increase of velocity ratio parameter B, Eckert number E_c, Magnetic parameter M, Prandtl number P_r and thermal radiation parameter R except Casson parameter β and porous matrix K_p. Thus it is concluded that non-Newtonian parameter and the presence of porous matrix reduce the rate of heat transfer at the bounding surface on which the flow phenomena occurs.

Table 3: Skin friction and Nusselt number at the plate

B	E_c	M	K	P_r	B	R	$f''(0)$	$-\theta'(0)$
0.1	0	0	10	0.71	0.1	1	-0.9061484	0.28598657
0.1	0.2	0	10	0.71	0.1	1	-0.9061484	0.28598657
0.1	0.2	0.5	10	0.71	0.1	1	-0.9262399	0.30087789
0.1	0.2	0.5	0.1	0.71	0.1	1	-0.360191	0.39828737
0.1	0.2	0.5	10	1	0.1	1	-0.92624	0.37802938
0.1	0.2	0.5	10	0.71	2	1	-2.5082692	0.21569436
0.1	0.2	0.5	10	0.71	0.1	3	-0.92624	0.21569436
2	0.2	0.5	10	0.71	0.1	1	1.14899708	0.80192012
2	0.2	0.5	0.1	0.71	0.1	1	0.65106272	0.75822076
0.1	0.2	0.5	0.1	0.71	0.1	1	-0.360191	0.39828737

5 Conclusions

The non-Newtonian property of Casson fluid is responsible for diffusing the momentum through more number of fluid layers. Slight change in magnetic field does not affect the velocity profile in both porous and nonporous media. The absence of magnetic field, Julian dissipation, and porosity of the medium lower down the temperature. The fluid with higher kinematic viscosity restricts the heat transfer to fewer layers of fluid. The straining rate and stretching rate have great influence on the flow criteria including stability and growth of boundary layer. Casson fluid parameter along with other parameters reduce the skin friction, which is desirable, except Eckert number E_c, which has no significant contribution. The non-Newtonian parameter and the presence of porous matrix reduce the rate of heat transfer at the bounding surface.

Acknowledgement

The authors are grateful to the anonymous referee for a careful checking of the details and for helpful comments that improved this paper.

References

[1] L.J. Crane, Flow past a stretching plate, ZAMP, **21**, 645-655 (1970).
[2] P. Caragher, L.J. Crane, Heat transfer on a continuous stretching sheet, Z Angew, Math mech, **62**, 564-573 (1982).
[3] H. Schlichting, K. Gersten, Boundary Layer Theory, Springer, Verlag, (2000); 110.
[4] P.D. Ariel, T. Hayat, S. Ashgar, The flow of an elastico-viscous fluid past a stretching sheet with partial slip, Acta Mechanica, **187**, 29–35 (2006).
[5] S. Nadeem, A. Hussain, M.Y. Malik, T Hayat, Series solutions for the stagnation flow of a second-grade fluid over a shrinking sheet, Applied Mathematics and Mechanics, **30**(10), 1255-1262 (2009).
[6] S. Nadeem, A. Hussain, M. Khan, Stagnation flow of a Jeffrey fluid over a shrinking sheet, Z. Naturforsch., **65a**, 540-548 (2010).
[7] T. Hayat, M. Qasim, Radiation and magnetic field effects on the unsteady mixed convection flow of a second-grade fluid over a vertical stretching sheet, International Journal of Numerical Methods in Fluids, **66**(7), 820-832 (2010).
[8] S. Nadeem, N. Faraz, Thin film flow of a second-grade fluid over a stretching/shrinking sheet with variable temperature-dependent viscosity, Chinese Physics Letters, **27**(3), 034704 (2010).
[9] S.R. Mishra, S. Baag, D.K. Mohapatra, Chemical reaction and Soret effects on hydromagnetic micropolar fluid along a stretching sheet, Engineering Science and Technology, an International Journal, **19**(4), 1919–1928 (2016).
[10] R.S. Tripathy, S.R. Mishra, G.C. Dash, M.M. Hoque, Numerical analysis of hydromagnetic micropolar fluid along a stretching sheet with non-uniform heat source and chemical reaction, Engineering Science and Technology, an International Journal, **19**(3), 1573–1581 (2016).
[11] G.C. Dash, R.S. Tripathy, M.M. Rashidi, S.R. Mishra, Numerical approach to boundary layer stagnation-point flow past a stretching/shrinking sheet, Journal of Molecular Liquids, **221**, 860–866 (2016).
[12] K. Ahmad, R. Nazar, Magnetohydrodynamic three-dimensional flow and heat transfer over a stretching surface in a viscoelastic fluid, Journal of science and technology **3**(1), 1–14 (2011).
[13] S. Nadeem, R.U. Haq, C. Lee, MHD flow of a Casson fluid over an exponentially shrinking sheet, Scientia Iranica **19**, 1550-1553 (2012).
[14] S.R. Mishra, G.C. Dash, M. Acharya, Mass and heat transfer effect on MHD flow of a viscoelastic fluid through porous medium with oscillatory suction and heat source, International Journal of Heat and Mass Transfer, **57**(2), 433–438 (2013).
[15] M. Turkyilmazoglu, I. Pop, Exact analytical solution for the flow and heat transfer near the stagnation-point on a stretching/shrinking sheet in a Jeffrey fluid, International Journal of Heat and Mass Transfer, **57**(1), 82-88 (2013).
[16] T.C. Chiam, Stagnation-point flow towards a stretching plate, Journal of the Physical Society of Japan, **63**, 2443–2444 (1994).
[17] K. Hiemenz, Die Grenzschicht an einem in den gleichformingen Flussigkeitsstrom einge-tauchten graden Kreiszylinder, Dingler's Poly. J., **326**, 321-324 (1911).
[18] T.R. Mahapatra, A. S. Gupta, Magnetohydrodynamic stagnation-point flow towards a stretching sheet, Acta Mechanica, **152**, 191-196 (2001).

[19] T. R. Mahapatra, A. S. Gupta, Heat transfer in stagnation-point flow towards a stretching sheet, Heat and Mass Transfer, **38**, 517?-521 (2002).
[20] A.G. Fredrickson, Principles and Applications of Rheology, Prentice- Hall, Englewood Cliffs, NJ, USA, 1964.
[21] M. Mustafa, T. Hayat, I. Pop, A. Aziz, Unsteady boundary layer flow of a Casson fluid due to an impulsively started moving flat plate, Heat Transfer, **40** (6), 563-576 (2011).
[22] K. Bhattacharyya, T. Hayat, A. Alsaedi, Exact solution for boundary layer flow of Casson fluid over a permeable stretching/ shrinking sheet, ZAMM?Journal of Applied Mathematics and Mechanics/Zeitschrift fr Angewandte Mathematik und Mechanik **94**(6), 522–528 (2014).
[23] K. Bhattacharyya, T. Hayat, A. Alsaedi, Analytic solution for magnetohydrodynamic boundary layer flow of Casson fluid over a stretching/shrinking sheet with wall mass transfer, Chinese Physics B, **22**, Article ID 024702 (2013).
[24] D. Bhukta, G.C. Dash, S.R. Mishra, Heat and mass transfer on MHD flow of a Viscoelastic fluid through porous media over a shrinking sheet, International Scholarly Research Notices, **2014**, Article ID 572162 (2014).
[25] M. H. Abolbashari, N. Freidoonimehr, F. Nazari, M.M. Rashidi, Entropy analysis for an unsteady MHD flow past a stretching permeable surface in nano-fluid, Powder Technology **267**, 256-267 (2014).
[26] M. M. Rashidi, M. Ali, N. Freidoonimehr, B. Rostami, M.A. Hossain, Mixed Convective Heat Transfer for MHD Viscoelastic Fluid Flow over a Porous Wedge with Thermal Radiation, Advances in Mechanical Engineering, **2014**, Article ID 735939 (2014).
[27] M.M. Rashidi, E. Erfani, Analytical method for solving steady MHD convective and slip flow due to a rotating disk with viscous dissipation and Ohmic heating, Engineering Computations, **29**(6), 562–579 (2012).
[28] N. Freidoonimehr, M.M. Rashidi, S. Mahmud, Unsteady MHD free convective flow past a permeable stretching vertical surface in a nano-fluid, International Journal of Thermal Sciences, **87**, 136–145 (2015).
[29] S. Abbasbandy , T. Hayat , A. Alsaedi , M.M. Rashidi, Numerical and analytical solutions for Falkner-Skan flow of MHD Oldroyd-B fluid, International Journal of Numerical Methods for Heat and Fluid Flow, **24**(2), 390–401 (2014).
[30] R.K. Dash, K.N. Mehta, G. Jayaraman, Casson fluid flow in a pipe filled with a homogeneous porous medium. International Journal of Engineering Science, **34**(10), 1145-1156 (1996).
[31] Y.C. Fung, Bio-dynamics circulation. New York Inc: SpringerVerlag; 1984.
[32] R. Nazar, N. Amin, D. Filip, I. Pop, Unsteady boundary layer flow in the region of the stagnation-point on a stretching sheet, International journal of engineering science, **42**, 1241–1253 (2004).
[33] K. Bhattacharyya, MHD Stagnation-point flow of Casson fluid and Heat Transfer over a Stretching sheet with Thermal Radiation, Journal of Thermodynamics,**2013**, 169674 (2013).

Satya Ranjan Mishra is the assistant professor in the Department of Mathematics, University of Karachi. His research interest include the areas of Computational ?uid Dynamics, Modeling and Simulation, Fluid Mechanics, and Numerical Simulation. He has published more than 40 refereed journal papers.

Asmat Ara obtained the Ph. D. degree from University of Karachi. She is the assistant professor in the Department of Computer Science, Mohammad Ali Jinnah University, Karachi. Her research interest include the areas of Nonlinear system, Approximate analytical methods, Fluid Mechanics, differential equations of applied mathematics, and theoretical analysis. She has published more than 30 refereed journal papers.

Najeeb Alam Khan obtained the Ph. D. degree from University of Karachi in 2013. He is the associate professor in the Department of Mathematics, University of Karachi. His research interest include the areas of Nonlinear system, Numerical methods, Approximate analytical methods, Fluid Mechanics, differential equations of applied mathematics, fractional calculus, fractional differential equation and theoretical analysis. He has published more than 110 refereed journal papers.